FACTA UNIVERSITATIS (NIŠ)
SER.: ELEC. ENERG. vol. 16, Dec. 2006, 231-237

Voltage Sag Drop in Speed Minimization in Modern Adjustable Speed Drives

Milutin P. Petronijević, Borislav I. Jeftenić, Nebojša M. Mitrović, and Vojkan Z. Kostić

Abstract: This paper researches behavior of rotor field oriented (RFO) and direct torque controlled (DTC) drives in speed controlled application in voltage sags circumstances. Problems in application will be able to appear, especially in work cases with speed and torque close to rated, even in a case when typical voltage tolerance curves show no drive trips. To overcome appeared drop in speed it was posed a field weakening algorithm during voltage sag. Analytic calculation and numerical simulation were presented in detail in this work. Knowing delay in RFO flux response and prompt DTC flux recall, methods for dynamic performance improving were advised.

Keywords: Adjustable speed drives, power quality, voltage sag, drop in speed, direct torque control, flux vector control.

1 Introduction

The fact that adjustable speed drives (ASD) with induction motors are highly sensitive to voltage sags can cause long re-start delays and production losses. An extra increase of expenses (for example in continuous processes as paper industry, glass production, etc.) caused by ASD voltage sags sensitivity which also leads to a numerous experimental and simulation studies ([1], [2]). The main aim of the studies mentioned above is to determine the sensitivity factors, and to propose prevention of the ASD's from tripping as a result of voltage sags.

The appearance of the speed drop during voltage dip was noticed in experimental ASD testing ([3]). In [1] it was presented drop in speed simplified analysis

Manuscript received February 7, 2006. Earlier version of this paper presented at IEEE ISIE 2005, June 20-23, 2005, Dubrovnik, Croatia.

M.P. Petronijević, N.M. Mitrović, and V.Z. Kostić are with Faculty of Electronic Engineering, A. Medvedeva 14, 1800 Nis, Serbia & Montenegro (e-mail: milutin@elfak.ni.ac.yu). B.I. Jeftenić is with Faculty of Electrical Engineering, Kralja Aleksandra 73, 11000 Belgrade, Serbia & Montenegro (e-mail: jeftenic@etf.bg.ac.yu).

based on energy balance equation. In cases of modern ASD it has nearly no paper presenting accurate criteria and defining drop in speed relation and the control performances loss. Nowadays converters with Field Oriented Control (FOC) and Direct Torque Control (DTC) for high performance AC drives in industrial application are mostly used. Reference [4] turns attention to torque reduction and drop in speed during voltage sag and advises field weakening and appropriate under-voltage protection adjusting, neglecting stator resistance and without strictly mathematical consideration.

In previous paper [5] the authors proposed few algorithms to overcome the drop in speed under voltage dip, but no exact definition was done. Field weakening during voltage sag was demonstrated as efficient method of drop in speed minimization. Control algorithms in RFO and DTC drives can be simple modified to maintain speed drop at a minimum. Very good dynamic performances are found in regard to speed drop in both speed closed loop ASD's.

This paper is an approaching one to the explanation of the solution mentioned above where the analytic relations were found out. The following lines will explain this paper organization. The Second section shows the basic stimulus for paper initiation and gives outlines for converter limitation in practice. The third section concretes outcomes in FOC drives, while in the fourth section the same ones are presented for DTC drives.

In Section V, the dynamic features are presented based on the complete electric drives model including control circuit and voltage sag generator to validate the drawn conclusions. Also, the different methods of the improvement of speed drop minimization are shown.

2 ASD voltage sag sensitivity

There are three reasons ([1]) for tripping ASD's because of voltage sag. The first one is that the control electronics power supply, regularly supplied by DC link voltage, also sensitive to voltage sag. If the power supply cannot obtain adequate voltage for the control electronics, the drive has to be shut down as a safety measure against losing control of the drive.

The second reason is union of under-voltage and/or over-current protection. If the DC link capacitor discharges its energy and the DC link voltage reaches the minimum allowed value (V_{DCmin}) under-voltage protection will be activated. This minimum level can be adjusted in the range from 65-70% up to 85-90% of rated DC link voltage. DC voltage drop under minimum level can lead to the appearance of the high inrush input current when the power-up again. Minimum DC bus voltage depends on maximum diode bridge current, i.e. DC bus charging circuit limitation.

The third reason is that some processes with multi-motor ASD (for example dried section of the paper machine with speed synchronized drives and load sharing ([6]) cannot tolerate the loss of accurate speed or torque control, even for a few seconds due to damage the final product or halt of the process.

In numerous papers ASD's voltage sag sensitivity is investigated in details, where the first two mentioned reasons are taken into consideration. In Fig. 1 typical voltage sag sensitivity curve was presented.

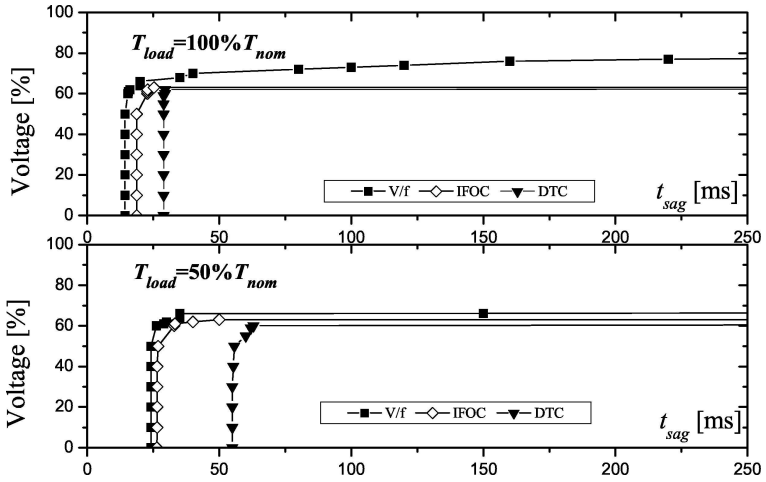

Fig. 1. Sensitivity of ASD drives to symmetrical three-phase sags with different load torque values: $T_{load} = 100\%T_{nom}$ (top); $T_{load} = 50\%T_{nom}$ (bottom)

The vertical parts of the drive voltage-tolerance curves are determined under-voltage protection response. Small difference between drives is the consequence of different DC voltage ripple and motor electromagnetic torque (stator currents) during sag. If the supply voltage recovers before the DC bus voltage reaches the under-voltage protection level, a high charging current is drawn from the supply network and may blow the fuses. If this possible, high inrush current can flow to induction motor and activate over-current protection. In V/Hz drive, horizontal part of the voltage-tolerance curve represents this effect. High performance drives (FOC and DTC) have controlling torque or current and high inrush current can't flow to induction motor without control. If inverter overload, modern drives have possibility to program different actions: to retain maximum available torque, decrease switching and output frequency with or without trip.

Drive manufactures declare that the usual input voltage range is $U_n \pm 10\%$. The possibility of faultless drive operation in input voltage range between minimum (corresponding to V_{DCmin}) and lower nominal voltage limit ($90\%U_n$) is main attraction for this paper.

Limits as consequences of PWM converter maximum output current (I_{max}) and maximum output voltage (U_{max}) can be represented in relation to the appropriate stator quantity through the following equations:

$$i_{qs}^2 + i_{ds}^2 \leq I_{\max}^2 \tag{1}$$

and

$$u_{qs}^2 + u_{ds}^2 \leq U_{\max}^2. \tag{2}$$

Maximum output current is determined by maximum continuous current of inverter semiconductor switches or induction motor rated current, i.e. maximum allowable thermal capacity of the converter or induction motor.

The maximum stator voltage depends on the available DC-link voltage V_{DC} and pulsewidth modulation (PWM) strategy ([7], [8]). In this paper, PWM strategy based on voltage space vector (SVPWM) is used, and then the output phase voltage on converter terminals, neglecting voltage drop on switches, is:

$$u(t) = (V_{DC}/2) \cdot m \cdot \sin(\omega t + \varphi) \tag{3}$$

Maximum possible modulation index m_{max} in linear modulation range is $2/\sqrt{3}$. If assuming that in front of converter is diode rectifier which is connected to the three-phase network with voltage magnitude V, maximum magnitude of the output voltage will be:

$$U_{\max} = (3/\pi) \cdot V \tag{4}$$

In practice, industrial frequency converters have different overmodulation methods, so in simulation model it has to be taken into consideration. If overmodulation is used, for example as in [9], it can be supposed that output voltage reconstruct input one in complete.

3 RFO controlled drives under voltage sag

Under the assumptions of linear magnetic circuit and balanced operating conditions, the equivalent two-phase model of the symmetrical induction motor, represented in the synchronous rotating reference frame, is:

$$\begin{bmatrix} u_{ds} \\ u_{qs} \end{bmatrix} = \begin{bmatrix} R_s & 0 \\ 0 & R_s \end{bmatrix} \begin{bmatrix} i_{ds} \\ i_{qs} \end{bmatrix} + \begin{bmatrix} p & -\omega_s \\ \omega_s & p \end{bmatrix} \begin{bmatrix} \lambda_{ds} \\ \lambda_{qs} \end{bmatrix} \tag{5}$$

$$\begin{bmatrix} 0 \\ 0 \end{bmatrix} = \begin{bmatrix} R_r & 0 \\ 0 & R_r \end{bmatrix} \begin{bmatrix} i_{dr} \\ i_{qr} \end{bmatrix} + \begin{bmatrix} p & -\omega_r \\ \omega_r & p \end{bmatrix} \begin{bmatrix} \lambda_{dr} \\ \lambda_{qr} \end{bmatrix}. \tag{6}$$

In the above equations, p represents the differential operator, ω_r - slip angular velocity ($\omega_r = \omega_s - \omega$), ω_s - synchronous reference frame speed and ω - rotor angular speed.

The flux equations are:

$$\begin{array}{l} \lambda_{ds} = L_s i_{ds} + L_m i_{dr}, \lambda_{qs} = L_s i_{qs} + L_m i_{qr} \\ \lambda_{dr} = L_r i_{dr} + L_m i_{ds}, \lambda_{qr} = L_r i_{qr} + L_m i_{qs} \end{array}. \tag{7}$$

Electromagnetic torque can be calculated using the following formula:

$$T_e = \frac{3}{2} P \frac{L_m}{L_r} (i_{qs}\lambda_{dr} - i_{ds}\lambda_{qr}) \tag{8}$$

Aligning the reference frame d-axis with rotor flux linkage phasor, will gain:

$$\lambda_{qr} = 0, \lambda_{dr} = \lambda_r \tag{9}$$

In steady state, all quantity differences will be zero, and can be counted that $i_{dr} = 0$, and:

$$T_e = c_1 i_{ds} i_{qs} \tag{10}$$

where $c_1 = \frac{3}{2} P \frac{L_m^2}{L_r}$.

It should be mentioned that in case the condition (9) introduction is not predicted the drive control method, so simplified equations (5)-(8), under condition (9) are with generalized meaning. When current limit is reached, the torque will be counted by the help of:

$$T_{e\_Imax} = c_1 \cdot i_{ds} \sqrt{I_{\max}^2 - i_{ds}^2} \tag{11}$$

In rotor field oriented (RFO) control, rotor flux magnitude λ_r controlled directly by d-component stator current i_{ds}:

$$\lambda_r = i_{ds} \frac{L_m}{1 + pT_r} \tag{12}$$

In base speed region it is possible to operate with constant rotor flux amplitude where the flux is adjusted at the rated value or at any arbitrary value which is appropriate for peak torque or efficiency. To achieve RFO control for set speed value, angular frequency of the stator variables should be:

$$\omega_s = \omega + \frac{R_r}{L_r} \frac{L_m}{\lambda_{dr}} i_{qs} \tag{13}$$

where the coordinate transformations are accomplished based on electrical angle:

$$\theta_e = \int \omega_s dt \tag{14}$$

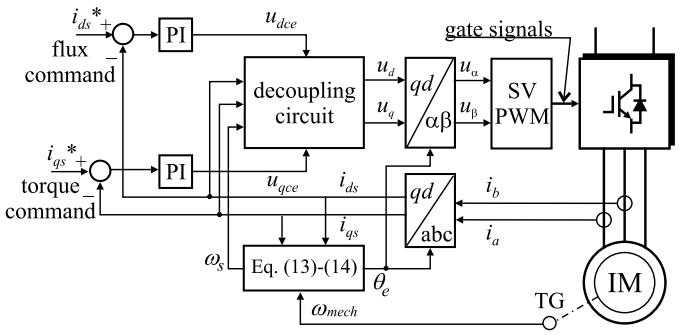

Fig. 2. Basic RFO control scheme (adopted from [10])

Basic scheme for induction motor RFO control is shown in Fig. 2.

Equation (2) in steady state and voltage limit condition, having in mind the relationships (5)-(7); can be written as ([11]):

$$Ai_{ds}^2 + Ci_{qs}^2 + Bi_{ds}i_{qs} \leq U_{\max}^2 \tag{15}$$

where: $A = R_s^2 + \omega_s^2 L_s^2$; $B = 2R_s\omega_s\frac{L_m^2}{L_r}$; and $C = R_s^2 + \omega_s^2\sigma^2 L_s^2$.

This voltage-limit boundary given by (15) is an ellipse which area and angle of major axis depend on voltage and frequency. Equation (1) in the same axis system explains a circle, so range of drive operation can be found in cross section of these two ones.

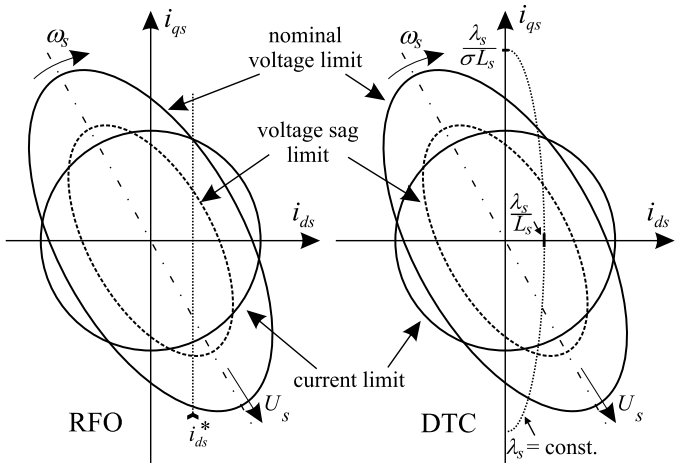

Fig. 3. Voltage and current limit under nominal and voltage sag conditions

For induction motor parameters done in Appendix, value of λ_r is calculated solving (5)-(7) in steady state at the motor breakdown torque and slip values which

result in maximum torque per ampere value ([12]). Appropriate value *d*-axis reference current (further named as ”breakdown value”) is given as:

$$i_{ds}^{*} = \lambda_r / L_m \tag{16}$$

and drawn in Fig. 3. In voltage dip case, based on (15), new ellipse can be drawn responding to reduced voltage limit where is easily noticeable decreasing of maximum possible *q*-axis stator current component which corresponds to electrical torque reduction. For constant load torque this leads to the speed regulation loss, which explicitly explains if we build adequate torque-speed characteristics in this case.

Considering that RFO control is ideal one (actual values follow the commanded ones completely), maximum torque under current limit based on (11) will be:

$$T_{e\_Imax}^{(RFO)} = c_1 \cdot i_{ds}^{*} \sqrt{I_{\max}^2 - i_{ds}^{*2}}. \tag{17}$$

The last equation, for motor parameters in Appendix results in line which is drawn in Fig. 4. and named as ”current limit”.

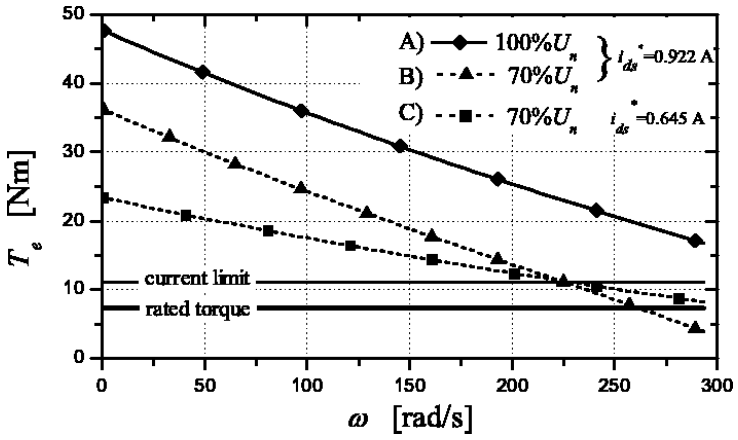

Fig. 4. Maximum torque under voltage and current limit

Replacing (13) and (16) in (15), finding out $i_{qs}(\omega, U_{\max}, i_{ds}^{*})$ and final changing in (10) we achieve torque-speed characteristics for RFO controlled drives under voltage limit (i.e. RFO controlled drive maximum torque under voltage limit):

$$T_{e\_Umax}^{(RFO)} = c_1 \cdot i_{ds}^{*} i_{qs}(\omega, U_{\max}, i_{ds}^{*}). \tag{18}$$

Solving (18) numerically, curves corresponding to maximum torque achieved respecting voltage limit existing. Curve named A outlined for nominal stator voltage and stator flux generating current calculated for peak torque under rated voltage. Curve B was obtained at voltage dip where remaining voltage is 70%U_n. Drive

working under the load and speed close to nominal values will result in loss of the adjusted speed. If i_{ds} is matched to magnitude close to 70%U_n and breakdown slip we can obtain curve C. It can be seen that under such a reduced voltage desired speed is retained because the IM develops torque nearly rated.

Changing i_{ds}^* results in maximum torque under current limit (17) shifting, so in case that is lower than value from (18), optimal i_{ds}^* value has to be calculated from equality (17) and (18). For example, when remaining dip voltage is 80%U_n we calculated $i_{ds}^* = 0.826$A, which prohibit the current limit to reduce maximum possible torque during voltage sag.

The proposed algorithm (field weakening in voltage dip regime) is simple for implementation in existing lookup table which is usually used for flux bringing in field weakening region. Knowing that rotor flux variation is characterized by the rotor time constant T_r, according to (12), optimization of dynamic torque response is eligible which can be presented in Section V. In this paper we use field weakening based on rotor angular speed as reported in [10], though it should be mentioned that industrial frequency converters usually use the field weakening method based on actual output frequency ([13]).

4 DTC drives under voltage sag

The Direct Torque Control (DTC) method usually uses a stator reference model of the induction motor for its implementation, avoiding the trigonometric operations of 3 phase to 2 phase transformation as in case synchronous reference frame. The implementation of the DTC scheme requires flux linkages and torque computations and generation of switching states through a feedback control of the torque and flux directly without inner current loops. The DTC method uses feedback control of torque and stator flux, which are computed based on DC link voltage and switch states (or on measured stator voltages) and motor currents. Basic DTC scheme is shown in Fig. 5, at which the optional speed feedback can be utilized in flux and torque estimator. Explanation about DTC and its modeling can be found in [14] in details.

Accepting that the DTC is ideal and that stator flux magnitude λ_s^* remains constant and equal to the proposed one, in synchronous reference frame can be added the following one:

$$\sqrt{(\lambda_{ds})^2 + (\lambda_{qs})^2} = \lambda_s^*. \tag{19}$$

Having in mind (7) and $i_{dr} = 0$ the last equation can be written:

$$(L_s i_{ds})^2 + (\sigma \cdot L_s \cdot i_{qs})^2 = (\lambda_s^*)^2. \tag{20}$$

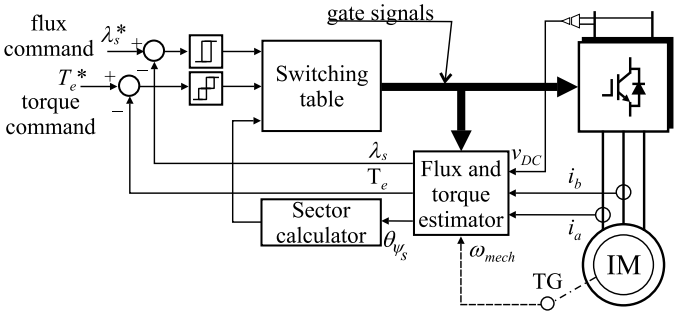

Fig. 5. Basic DTC scheme

Solving the last equation for motoring regime operation leads to:

$$i_{ds} = \sqrt{(\lambda_s^*)^2 - \sigma^2 \cdot L_s^2 \cdot i_{qs}^2}/L_s. \tag{21}$$

Trajectory described by (21) was drawn in Fig. 3 accomplished by appropriate contours corresponding to (1) and (15). It is able to notice that there are differences in behavior of the RFO controlled and DTC drives under voltage dip condition, even in case of identical frequency converter power section.

Substitution (21) into (10) gives the torque in DTC drive:

$$T_e = \frac{c_1}{L_s} i_{qs} \sqrt{(\lambda_s^*)^2 - \sigma^2 \cdot L_s^2 \cdot i_{qs}^2} \tag{22}$$

The maximum value of (22) is:

$$T_{e\max}^{(DTC)} = \frac{c_1}{2} \frac{(\lambda_s^*)^2}{\sigma L_s^2}. \tag{23}$$

This value presents maximum possible DTC drive torque if voltage and current limits are not taken into account. Such limitation does not exist in RFO controlled drives.

Maximum torque value, if the stator current magnitude is constrained by the maximum power converter output current I_{max}, can be found by combining (21), (1) and (11), which leads us to:

$$T_{e\_Imax}^{(DTC)} = \frac{c_1[(L_s^2 I_{\max}^2 - \lambda_s^2)(\lambda_s^2 - \sigma^2 L_s^2 I_{\max}^2)]^{1/2}}{(1-\sigma^2)L_s^2} \tag{24}$$

The value given in (24) exists if it is less than $T_{e\max}^{(DTC)}$. The previous equation, for motor parameters in Appendix is presented graphically in Fig. 6 and also named ”current limit”.

Considering (22) under circumstances from (13) the maximum torque values can be found which are presented in Fig. 6 (curve A). Value λ_s^* was adjusted in away to obtain maximum torque value at rated voltage and speed. At voltage dip with remaining voltage of 70%U_n (curve B) was obtained in the same way. If s is reduced to 70% of the previous value, it can be resulted in curve C. By such a way induction motor was led to develop nearly rated torque.

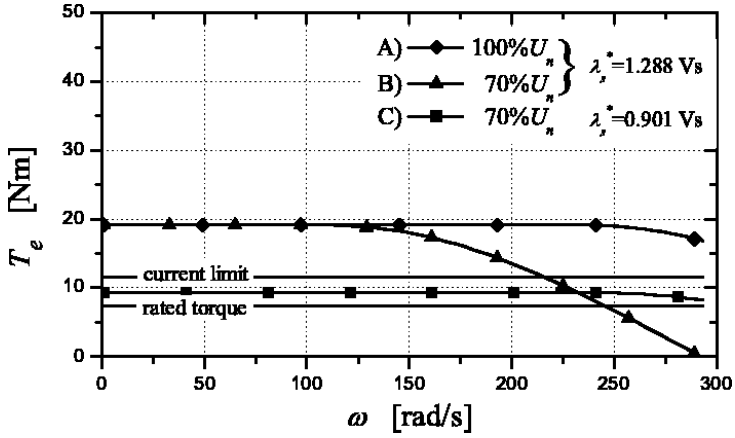

Fig. 6. Maximum torque under voltage and current limit in rated voltage and voltage sag cases

Similar to the RFO controlled drives, according to (23) and (24), changing flux value λ_s^* results in changing limit values given in this equations. Due to limited space, in this paper finding optimal flux value respecting to voltage and current limit will not be considered.

Stator flux changing at DTC drives is direct controlled by changing stator voltage ([15]). This fact simplifies implementation of voltage sag field weakening algorithm comparing to RFO drives.

5 Results

The fact that drives are more sensitive regarding drop in speed working under load and speed close to nominal ones can be important for industrial users. If a working speed is adjusted at a value where voltage limit (V_{DCmin}) causes no reduction of maximum possible torque, the drive doesn't register drop in speed during voltage sag regime. Complete speed controlled drive model including RFO control and DTC were conducted by using Matlab/Simulink simulation package ([5]).

For motor data in Appendix, $V_{DC} = 70\%V_{DCnom}$ and for given values i_{ds}^*, and for λ_s^* previous fact was shown in Fig. 7. From this point of view, industrial multi-

motor drives consumers have possibility to predict such an operational drives speed which is insensitive to voltage sag. The other possibility is to reduce working speed at the speed mentioned above in case when voltage sag appears, or DC link voltage reduces.

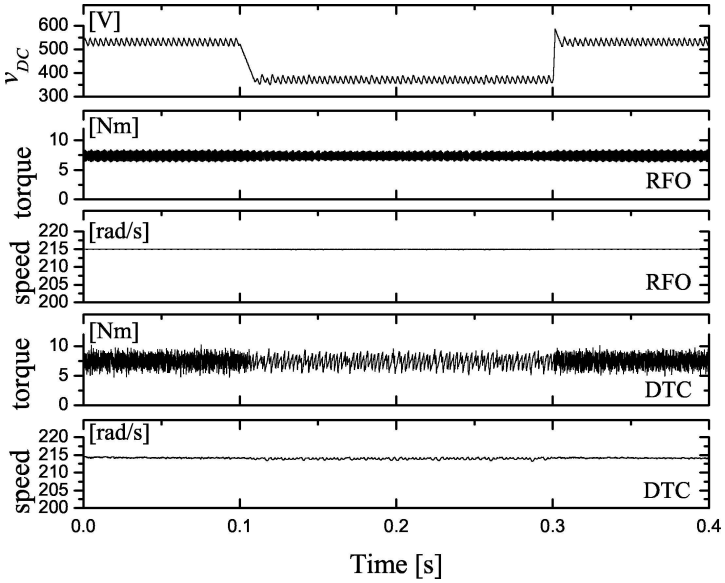

Fig. 7. Insensibility illustration at voltage sag with reduced working speed

The optional method for drop in speed overcoming was shown in this paper, where we should know features of each drives. In ASD with RFO the problem of adequate adjusting flux-producing stator current component appeared. Before voltage sag, this component is equal to breakdown value i_{ds}^*, as in the period after voltage dropping.

During the voltage sag flux-producing current component can be adjusted according to the following rules: method 1) value with no change; 2) the value which is appropriate to DC bus voltage value during the sag based on (17) and (18); 3) the dynamic *d* and *q*-axis current sharing strategy which obtains higher transient torque and minimum speed deviation, knowing delay in flux response. The maximum available current I_{max} is to be distributed into *d* and *q*-axis current. The algorithm that is developed here is characterized with the following rules:

$i_{ds}^* = 0$	$i_{qs}^* = I_{\max}$ for $0 < t < t_1$
i_{ds}^* from Eq. (17) and (18)	$i_{qs}^* = \sqrt{I_{\max}^2 - i_{ds}^{*2}}$ for $t_1 < t < t_2$

where: t_1 is the time when the rotor flux λ_r drops to the decreased value which

is matched with the sagged DC bus voltage, t_2 is the time of the power-up. After sag ending ($t > t_2$), flux-producing current component resets to the breakdown value.

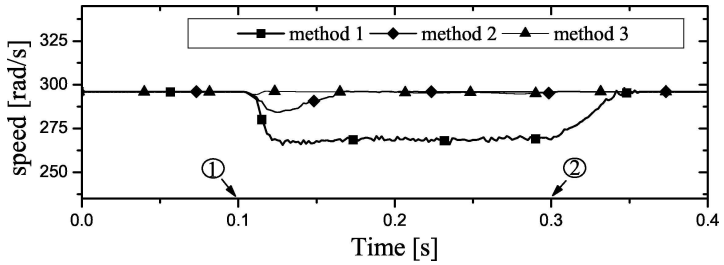

Fig. 8. Motor speed drop during voltage sag in drive with RFO (1- point of sag start, 2- point of sag end): $U_{sag} = 70\%U_n$

In Fig. 8 is presented the comparison of the simulation results, for three methods mentioned above, in case of symmetrical three-phase voltage sag. Developed simulation model takes into account sampling times and frequency bandwidths for currents and voltages measurement loops. As it can be seen in Fig. 8, the proposed method of the dynamic current sharing of the inverter maximum current, leads to the minimum speed drop. The adjustable speed drive with RFO control where the third method is implemented reacts faster than the first two ones because of forcing torque-producing current component. Besides the fact that minimum drop in speed was occurred, it should be stated that minimum speed recovery time was achieved.

We also emphasize that higher imposed current limit of the inverter enables improvement in drop in speed minimization, recovery of deeper voltage sag as well.

The differences in behavior of the drives with RFO control and DTC were illustrated in Fig. 9 for voltage sag with remaining voltage of $80\%U_n$. It's clearly seen that RFO controlled drives won't be sensitive to voltage sag, while DTC drives have minor drop in speed as can be seen in Fig. 10.

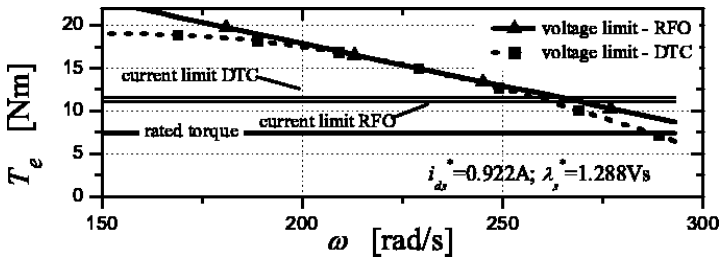

Fig. 9. Maximum torque comparison for $U_{sag} = 80\%U_n$ for RFO controlled and DTC drives

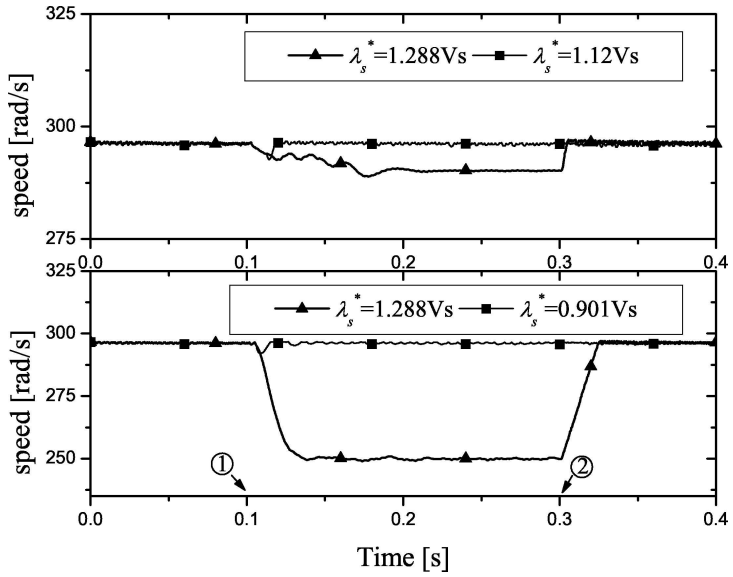

Fig. 10. Motor speed drop during voltage sag in drive with DTC (- point of sag start, - point of sag end): $U_{sag} = 80\%U_n$ (top); $U_{sag} = 70\%U_n$ (bottom)

In the case of ASD with DTC it is modeled very simple algorithm having in mind fast response of the controlled system when flux reference changes. In the simulation, λ_s^* is reached as output from look-up table with V_{DC} and as inputs. In Fig. 10 simulation results in drop in speed for DTC model (without stator flux correction) and for model in which flux weakening during voltage sag is implemented are shown.

Flux and torque hysteresis controller in DTC bring to excellent dynamic performances in transients. Response rapidity will be dominant determined by low-pass filter transfer function in DC-bus voltage measurement loop.

6 Conclusion

PWM inverter drives will shut down at voltage sag, initiated by their under-voltage or over-current protection scheme. Starting from steady-state analysis in this paper is also presented detailed derivation of the voltage sag influence on the drop in speed in RFO and DTC speed controlled drives. Regular control algorithms are able to cause the drop in speed which cannot be accepted in some industrial application.

According to the analytic relations it was proposed drive operation strategy at reduced speed when the drive is nearly insensible under voltage sag influence. The optional method is field weakening implementation during voltage sag. Control

algorithms in RFO controlled and DTC drives can be simply modified introducing DC link voltage feedback and affording field weakening under rated speed depending on voltage sag magnitude.

To minimize drop in speed at ASD with RFO control it was examined algorithm of dynamic current sharing of the inverter maximum current. At DTC drives prompt flux response lets simple field weakening algorithm implementation. Very good dynamic performances are found in regard to drop in speed in both speed closed loop ASD's.

Appendix: List of symbols and motor data

R_s – Stator resistance, 7.845Ω
R_r – Rotor resistance, 7.187Ω
L_{ls}, L_{lr} – Stator and Rotor Leakage Inductance, $31mH$
L_m – Magnetizing Inductance, $0.815H$
u_{sd}, u_{sq} – Direct and Quadrature axis Stator Voltages
i_{sd}, i_{sq} – Direct and Quadrature Stator Currents
i_{rd}, i_{rq} – Direct and Quadrature Rotor Currents
P – No. Pole Pairs, 1
P_n – Nominal Motor Power, $2200W$
U_n – Supply network rated line-line voltage rms value, $380V$
ω_n – Nominal rotor angular speed, $297rad/s$
σ – Total leakage coefficient, 0.049
T_r – Rotor time constant, $0.174s$
m – Modulation index

References

[1] M. H. J. Bollen and L. D. Zhang, "Analysis of voltage tolerance of ac adjustable-speed drives for three-phase balanced and unbalanced sags," *IEEE Trans. Ind. Applicat*, vol. 36, pp. 904–910, May/June 2000.

[2] S. Ž. Djokić, J. Milanović, K.Stockman, and R.Belmans, "Voltage-tolerance curves of PWM drives: comparison of simulations and measurements," in *Proc. 12th International symposium on Power electronics*, Novi Sad, Serbia and Montenegro, Nov. 2003, pp. T6–1.3.

[3] K. Stockman, F. D'hulster, K. Verhaege, M. Didden, and R. Belmans, "Ride-through of adjustable speed drives during voltage dips," *Electric Power Systems Research*, vol. 66, pp. 49–58, July 2003.

[4] K. Stockman, F. D'hulster, J. Desmet, and R. Belmans, "Torque behaviour of a field oriented induction motor drive towards voltage sag conditions," in *Proc. of papers - 10th IEEE/ICHQP*, Rio de Janeiro, Brasil, Oct. 2002.

[5] M. Petronijević, V. Kostić, N. Mitrović, , and B. Jeftenić, "Modern PWM drives voltage sags sensitivity," in *Proc. of papers - ICEST 2004*, Bitola, Macedonia, June 2004, pp. 663–666.

[6] B. Jeftenić, M. Krgović, and M. Bebić, "The selection of sectional drives for the replacement of the line shaft drive in a paper machine," *Cellulose chemistry and technology*, vol. 36, pp. 559–565, Sept./Oct. 2002.

[7] J. Holtz, "Pulsewidth modulation for electronic power conversion," *Proceedings of the IEEE*, vol. 82, pp. 1194–1214, Aug. 1994.

[8] K. Zhou and D. Wang, "Relationship between space-vector modulation and three-phase carrier-based PWM: a comprehensive analysis," *IEEE Trans. Ind. Electron*, vol. 49, pp. 186–196, Feb. 2002.

[9] A. Khambadkone and J. Holtz, "Compensated synchronous PI current controller in overmodulation range and six-step operation of space vector modulation based vector controlled drives," *IEEE Trans. Ind. Electron*, vol. 49, pp. 574–580, June 2002.

[10] P. Vas, *Sensorless vector and direct torque control*. New York: Oxford University Press, 1998.

[11] J. Chang and B. Kim, "Minimum-time minimum-loss speed control of induction motors under field-oriented control," *IEEE Trans. Ind. Electron*, vol. 44, pp. 809–815, Dec. 1997.

[12] F. Khater, R. Lorenz, D. Novotny, and K. Tang, "Selection of flux level in field-oriented induction machine controllers with consideration of magnetic saturation effects," *IEEE Trans. Ind. Applicat*, vol. 23, pp. 904–910, Mar./Apr. 1987.

[13] Siemens. (2004, June) Masterdrives user manual. [Online]. Available: http://www.siemens.com/masterdrives

[14] N. Mitrović, V. Kostić, M. Petronijević, and B. Jeftenić, "Simulation of direct torque control schemes for electric drive application, Part I," *Trans. on Automatic Control and Computer Science*, vol. 49, pp. 83–86, May 2004.

[15] D. Casadei, F. Profumo, G. Sera, and A. Tani, "FOC and DTC: two viable schemes for induction motors torque control," *IEEE Trans. Power Electron*, vol. 17, pp. 779–787, Sept. 2002.